Structural and Functional Models for the Dicopper Site in Hemocyanin. Dioxygen Binding by Copper Complexes of Tris(1-R-4-R′-imidazolyl-κN)phosphines

Will E. Lynch, Donald M. Kurtz, Jr.,* Shengke Wang, and Robert A. Scott

Contribution from the Department of Chemistry and Center for Metalloenzyme Studies, University of Georgia, Athens, Georgia 30602

Received June 1, 1994[⊗]

Abstract: Complexes of the type $[Cu^{I}(T1Et4RIP)]X$ (T1Et4RIP = tris(1-ethyl-4-R-imidazolyl)phosphine (R = methyl (Me), isopropyl (iPr)); X = PF_6, ClO_4, CF_3SO_3), in which T1Et4RIP functions as a tridentate nitrogen donor ligand, were prepared by Lewis acid-base reactions between $[Cu^{I}(CH_3CN)_4]X$ and T1Et4RIP in dry, degassed solvents. The colorless acetonitrile adducts, $[Cu^{I}(T1Et4RIP)(CH_3CN)]X$, were obtained by crystallization from acetontrile. The complex with R = iPr and X = PF_6 crystallizes in the space group $I2_13$ with $a = b = c = 18.912(2)$ Å and $Z = 8$. The refinement converged with a final R (R_w) value of 0.075 (0.098) for 988 reflections with $F > 3\sigma(F_o)$. The Cu^{I} is coordinated in a trigonally distorted tetrahedral fashion to three imidazolyl nitrogen atoms at 2.08 Å and one acetonitrile nitrogen atom at 1.90 Å . Exposure of dry solutions of these Cu^{I} complexes to O_2 below −60 °C resulted in an isolable purple species with spectroscopic and magnetic properties characteristic of (μ-η^2:η^2-peroxo)-dicopper(II) complexes. The representative complex analyzing for $\{[Cu(T1Et4MeIP)]_2(O_2)\}(PF_6)_2$ has the following approximate values: diamagnetic; UV-vis, 338 nm (ϵ = 19 000 M^{-1} cm^{-1}), 521 nm (ϵ = 1000 M^{-1} cm^{-1}); ν-(O-O), 740 cm^{-1}. The Cu X-ray absorption fine structure spectrum of this complex with X = ClO_4 was best fit with a Cu scatterer at 3.48 Å , two O (or N) scatterers at 1.94 Å, and two sets of N (or O) scatterers: two at 2.05 Å and one at 2.30 Å. These spectroscopic, magnetic, and structural properties are characteristic of (μ-η^2: η^2-peroxo)dicopper(II) complexes having a planar Cu_2O_2 core and terminal nitrogen donor ligands, including the dicopper site in oxyhemocyanin. The $[Cu^{I}(T1Et4RIP)(CH_3CN)]X$ complexes with R = iPr react with O_2 at −78 °C to produce dioxygen adducts with spectroscopic and magnetic properties very similar to those listed above for R = Me. The complexes with R = iPr, upon repeated thermal cycling between −78 and ≈−20 °C in methanol, exhibit *reversible* binding of dioxygen. This process can be readily monitored by the characteristic visible absorption spectrum of the dioxygen adduct. Thus, copper complexes of tris(imidazolyl)phosphines with 1,4-disubstituted imidazolyl groups have been successfully used to model spectroscopic, magnetic, structural, and functional properties of the dicopper site in hemocyanin.

Introduction

Among the synthetic challenges to bioinorganic chemists, few have received more attention recently than the dicopper active site of hemocyanin and its closely related counterpart in tyrosinase.[1] This interest has focused on their functional reactions with O_2, which lead to reversible O_2 binding (hemocyanin) or *ortho* hydroxylation of phenols (tyrosinase). In the case of hemocyanin, an X-ray crystal structure revealed that the two noninteracting Cu^{I} ions are each ligated by three imidazole side chains from histidine residues.[2] EXAFS[3] studies indicate a Cu···Cu distance of ≈3.6 Å in oxyhemocyanin.[4] Intriguing features of the oxyhemocyanin dicopper site include its diamagnetism, interpreted as due to strong antiferromagnetic coupling between the two Cu^{II} centers, two intense electronic absorptions at ≈340 nm (ϵ = 20 000 M^{-1} cm^{-1}) and ≈570 nm (ϵ = 1000 M^{-1} cm^{-1}), assigned to $O_2^{2-} \rightarrow Cu^{II}$ charge transfer transitions, and an unusually low O-O stretching frequency, ≈750 cm^{-1}, observed in the resonance Raman spectrum.[4] These properties have been interpreted according to equilibrium 1:

$$\underset{\text{deoxy}}{Cu^{I}\cdots Cu^{I}} + O_2 \leftrightarrow \underset{\text{oxy}}{Cu^{II}-(O_2^{2-})-Cu^{II}} \qquad (1)$$

Given the three histidyl ligands to each copper in hemocyanin, the use of tridentate nitrogen donor ligands would appear to be a promising approach to synthetic modeling. In 1984, $Cu^{I}(HB(3,5\text{-}Me_2pz)_3)(C_2H_4)$ was reported to react with O_2, yielding a purple solid which was formulated as a mononuclear Cu^{II} superoxo species.[5] Ethylene was found to displace the bound O_2, thereby regenerating the Cu^{I} complex. However, the mononuclear superoxo formulation has recently been questioned.[1c]

In a series of elegant papers,[6-11] Kitajima and co-workers showed that copper complexes of $HB(3,5\text{-}R_2pz)_3$ (R = Me, iPr,

[⊗] Abstract published in *Advance ACS Abstracts*, November 1, 1994.

(1) (a) Karlin, K. D.; Tyeklár, Z. *Adv. Inorg. Biochem.* **1994**, *9*, 123. (b) Karlin, K. D.; Tyeklár, Z.; Zuberbühler, A. D. in *Bioinorganic Catalysis*; Reedijk, J., Ed.; Marcel Dekker: New York, 1993; p 261. (c) Kitajima, N.; Moro-oka, Y. *Chem. Rev.* **1994**, *94*, 737.

(2) (a) Volbeda, A.; Hol, W. G. *J. Mol. Biol.* **1989**, *209*, 249. (b) Hazes, B.; Magnus, K. A.; Bonaventura, C.; Bonaventura, J.; Dauter, Z.; Kalk, K. H.; Hol, W. G. J. *Protein Sci.* **1993**, *2*, 597.

(3) Abbreviations used: EXAFS, extended X-ray absorption fine structure; T1R4R′IP, tris(1-R-4-R′imidazol-2-yl)phosphine (R and R′ listed in Scheme 1); $HB(3,5\text{-}Me_2pz)_3$, hydrotris(3,5-dimethylpyrazolyl)borate(1−); $HB(3,5\text{-}iPr_2pz)_3$, hydrotris(3,5-diisopropylpyrazolyl)borate(1−); Im, imidazolyl; Me, methyl; Et, ethyl; iPr, isopropyl; Ph, phenyl; tBu, *tert*-butyl.

(4) (a) Solomon, E. I.; Baldwin, M. J.; Lowery, M. D. *Chem. Rev.* **1992**, *92*, 521. (b) Solomon, E. I.; Tuczek, F.; Root, D. E.; Brown, C. A. *Chem. Rev.* **1994**, *94*, 827.

(5) Thompson, J. S. *J. Am. Chem. Soc.* **1984**, *106*, 4057.

(6) Kitajima, N.; Fujisawa, K.; Fujimoto, C.; Moro-oka, Y.; Hashimoto, S.; Kitagawa, T.; Toriumi, K.; Tatsumi, K.; Nakamura, A. *J. Am. Chem. Soc.* **1992**, *114*, 1277.

(7) Kitajima, N.; Koda, T.; Hashimoto, S.; Kitagawa, T.; Moro-oka, Y. *J. Chem. Soc., Chem. Commun.* **1988**, 151.

(8) Kitajima, N.; Koda, T.; Iwata, Y.; Moro-oka, Y. *J. Am. Chem. Soc.* **1990**, *112*,8833.

0002-7863/94/1516-11030$04.50/0

Scheme 1

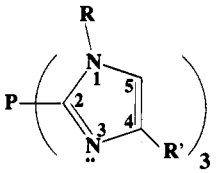

TIP: R = R' = H
TMeIP: R = H, R' = Me
T1,4DMeIP: R = R' = Me
T1Et4MeIP: R = Et, R' = Me
T1Et4iPrIP: R = Et, R' = iPr
T1Et4tBuIP: R = Et, R' = tBu

1: $[Cu^{I}(T1Et4MeIP)]^{+}$
2: $\{[Cu(T1Et4MeIP)]_2(O_2)\}^{2+}$
3: $[Cu^{I}(T1Et4iPrIP)(CH_3CN)]^{+}$
4: $\{[Cu(T1Et4iPrIP)]_2(O_2)\}^{2+}$

Ph) form peroxo-bridged dicopper(II) complexes at ≤ -20 °C which are spectroscopically and magnetically very similar to those reported for oxyhemocyanin. The X-ray crystal structure of $[Cu(HB(3,5\text{-}iPr_2pz)_3)]_2(O_2)$[6] unambiguously established the peroxo-bridging mode to be $\mu\text{-}\eta^2\text{:}\,\eta^2$ with a planar Cu_2O_2 geometry. This same O_2 bridging geometry has recently been confirmed in oxyhemocyanin.[12]

Kurtz et al. have used the tridentate imidazolyl donor ligands, TIP, TMeIP, and T1,4DMeIP (cf. Scheme 1) to assemble iron and manganese complexes and clusters as models for non-heme metal sites in proteins.[13-15] We have now extended the use of similar ligands to modeling of the hemocyanin active site. In this report, we describe the synthesis and characterization of Cu^{I} complexes of tris(imidazolyl)phosphine ligands containing 1,4-disubstituted imidazolyl groups and the reactions of these complexes with O_2. The use of imidazolyl rather than pyrazolyl ligands should in principle more closely model ligation of the dicopper site in hemocyanin.

Experimental Section

Materials and Methods. Preparations of Compounds. Reagents were obtained mainly from Aldrich Chemical Co. and used without further purification. Acetonitrile, dichloromethane and methanol were distilled from calcium hydride. Benzene and acetone were distilled over calcium chloride and P_2O_5, respectively. Tetrahydrofuran and diethyl ether were distilled from sodium/benzophenone. All anaerobic manipulations were carried out in either Schlenk-type glassware attached to a dry O_2-free Ar/vacuum manifold or in a dry, Ar-filled glove box. $[Cu^{I}(CH_3CN)_4]X$ complexes (X = PF_6, ClO_4, CF_3SO_3) were prepared via adaptation of a standard literature preparation.[16] T1Et4MeIP was prepared by a previously published procedure for T1,4DMeIP,[15] but substituting iodoethane for iodomethane. All copper complexes were found to be hygroscopic in solid form as well as in solution, and precautions to limit exposure to moisture and air were, therefore, exercised. Reactions conducted at −78 °C used a dry ice/acetone bath. Unless otherwise noted, all spectral data were obtained at ambient temperature (≈23 °C). O_2 gas (99 1/2% ^{18}O) was obtained from ICON Stable Isotopes, Mt. Marion, NY. Elemental analyses were performed by Atlantic Microlabs, Norcross, GA.

1-Ethyl-4-isopropylimidazole. 1-Bromo-3-methyl-2-butanone was prepared by a previously published procedure.[17] Procedures described by Sorrell et al.[18a] and by Jönsson[18b] for synthesis of 1,4-disubstituted imidazoles were modified as follows. 4-Isopropylimidazole was prepared by the reaction of 1-bromo-3-methyl-2-butanone (40.0 g) and formamide (150 mL). After the neat reaction mixture had been refluxed for 4 h, the system was cooled to room temperature and approximately 200 mL of 10% aqueous potassium carbonate was added to a pH of 9.5. The product was then extracted with 100 mL aliquots of chloroform until the brown organic layer faded to pale yellow. The organic fractions (approximately 500 mL) were combined and sequentially washed with 2 × 100 mL aliquots of 10% aqueous potassium carbonate and water. The organic layer was then dried over anhydrous sodium sulfate, and the solvent was removed under vacuum. The resulting brown oil, containing mostly 4-isopropylimidazole (11.4 g), was found to be sufficiently pure to carry through to the next step. (Further purification can be obtained by vacuum distillation to yield a pale yellow oil, if desired.) 1-Ethyl-4-isopropylimidazole was then prepared by equimolar reaction of ethyl iodide (16.2 g) and the crude 4-isopropylimidazole (11.4 g), as described previously.[19] The reaction produces a mixture of 1-ethyl-4- and -5-isopropylimidazole. The desired 1,4 isomer was obtained by vacuum distillation of this mixture and resulted in a yield of approximately 3.0 g. ^1H NMR ($CDCl_3$): δ 1.22 (d, 6H, CHMe_2), δ 1.40 (t, 3H, CH_2Me), δ 2.85 (sept, 1H, CHMe$_2$), δ 3.89 (q, 2H, CH_2Me), δ 6.59 (s, 1H, 5-*Im*), δ 7.36 (s, 1H, 2-*Im*).

T1Et4iPrIP. This compound was prepared by modification of a standard literature procedure[20] as follows. Under an argon atmosphere was placed 5.3 g of 1-ethyl-4-isopropylimidazole, and 100 mL of dry tetrahydrofuran was added. *n*-Butyllithium (15.6 mL, 2.5 M) was added dropwise with stirring over a period of 30 min. The reaction mixture was stirred for 1 h, at which time it was cooled to −78 °C. PCl_3 (1.7 g, 1.1 mL) was then added dropwise over 5 min, and the reaction was stirred at −78 °C for 4 h. The mixture was then filtered as rapidly as possible, while attempting to maintain a temperature of −78 °C, through a medium porosity glass frit which was open to the atmosphere. The collected white powder on the frit was then dissolved in 100 mL of chloroform at room temperature and the filtered solution was washed quickly with 2 × 100 mL of 10% aqueous sodium hydroxide. The organic layer was dried over sodium sulfate and filtered, and the solvent was removed under vacuum to yield 1.8 g of a white powder. ^1H NMR ($CDCl_3$) δ 1.05 (t, 9H, CH_2Me), δ 1.20 (d, 18H, CHMe_2), δ 2.87 (sept, 3H, CHMe$_2$), δ 4.03 (q, 6H, CH_2Me), δ 6.80 (s, 3H, *Im*). ^{31}P NMR (CD_3OD): δ -57.60. Exposure of a room-temperature solution of this product to air resulted in slow oxidation to the corresponding phosphine oxide. This oxidation was verified via ^{31}P NMR and reaction with hydrogen peroxide. No such oxidation was observed for the copper complexes described below.

$[Cu^{I}$(T1Et4MeIP)]X (X = PF_6, ClO_4, CF_3SO_3) (1-X). T1Et4MeIP (0.20 g, 0.56 mmol) was placed in a 100 mL Schlenk flask and charged with 15 mL of methanol. The resulting mixture was stirred until complete dissolution occurred (approximately 10 min). All subsequent manipulations were conducted anaerobically. In a separate flask, the cuprous salt, $[(Cu(CH_3CN)_4]X$ (0.56 mmol), was dissolved in 10 mL of methanol with stirring over the same period. This solution was then added via cannula to the ligand solution and stirred under argon for a period of 1 h. Dry diethyl ether was then added to a standing solution of the complex until a white precipitate was observed. This mixture was then stored for 12 h at −20 °C and the solid subsequently collected by filtration. **1**-PF_6. Yield: 0.22 g. Anal. Calcd for $CuC_{18}H_{27}N_6P_2F_6$: C, 38.12; H, 4.81; N, 14.82. Found: C, 38.16; H, 4.85; N, 14.75. ^1H NMR (CD_2Cl_2): δ 1.35 (t, 9H, CH_2Me), δ 2.24 (s, 9H, 4-*Me*), δ 4.24 (q, 6H, CH_2Me), δ 6.95 (d, 3H, *Im*). ^{31}P NMR

(9) Kitajima, N.; Koda, T.; Hashimoto, S.; Kitagawa, T.; Moro-oka, Y. *J. Am. Chem. Soc.* **1991**, *113*, 5664.
(10) Kitajima, N.; Fujisawa, K.; Moro-oka, Y.; Toriumi, K. *J. Am. Chem. Soc.* **1989**, *111*, 8975.
(11) Baldwin, M. J.; Root, D. E.; Pate, J. E.; Fujisawa, K.; Kitajima, N.; Solomon, E. I. *J. Am. Chem. Soc.* **1992**, *114*, 10421.
(12) (a) Magnus, K. A.; Hazes, B.; Ton-That, H.; Bonaventura, C.; Bonaventura, J.; Hol, W. J. G. *Proteins: Struct., Funct., Genet.* **1994**, *19*, 302. (b) Magnus, K. A.; Ton-That, H.; Carpenter, J. E. *Chem. Rev.* **1994**. *94*, 727.
(13) Wu, F. J.; Kurtz, D. M., Jr.; Hagen, K. S.; Nyman, P. D.; Debrunner, P. G.; Vankai, V. A. *Inorg. Chem.* **1990**, *29*, 5174.
(14) Wu, F. J.; Kurtz, D. M., Jr. *J. Am. Chem. Soc.* **1989**, *111*, 6563.
(15) Vankai, V. A.; Newton, M. G.; Kurtz, D. M., Jr., *Inorg. Chem.* **1992**, *31*, 341.
(16) Kubas, G. J. *Inorg. Synth.* **1979**, *19*, 90.
(17) Gaudry, M.; Marquet, A. *Org. Synth.* **1967**, *55*, 24.
(18) (a) Sorrell, T. N.; Allen, W. E. *J. Org. Chem.* **1994**, *59*, 1589. (b) Jönsson, A. *Acta Chem. Scand.* **1954**, *8*, 1389.
(19) Takeuchi, Y.; Yeh, H. J. C.; Kirk, K. L.; Cohen, L. A. *J. Org. Chem.* **1978**, *43*, 3565.
(20) Curtis, N. J.; Brown, R. S. *J. Org. Chem.* **1980**, *45*, 4038.

(CD_2Cl_2) δ −97.98, δ −38.65 (sept). UV−vis (dichloromethane, nm (M^{-1} cm^{-1})): 323 sh (4300). (**1**-ClO_4). Yield: 0.16 g. Anal. Calcd for $CuC_{18}H_{27}N_6PClO_4$: C, 41.46; H, 5.23; N, 16.12. Found: C, 41.23; H, 5.23; N, 16.11. ^1H NMR (CD_2Cl_2) δ 1.35 (t, 9H, CH_2*Me*), δ 2.24 (s, 9H, 4-*Me*), δ 4.24 (q, 6H, *CH_2*Me), δ 6.95 (d, 3H, *Im*). ^{31}P NMR (CD_2Cl_2): δ −98.88. UV−vis (dichloromethane, nm (M^{-1} cm^{-1})) 327 sh (5400). **1**-CF_3SO_3. Yield: 0.14 g. Anal. Calcd for $CuC_{18}H_{27}N_6PF_3SO_3$: C, 39.96; H, 4.78; N, 14.72. Found: C, 39.95; H, 4.76; N, 14.66. ^1H NMR (CD_2Cl_2): δ 1.44 (t, 9H, CH_2*Me*), δ 1.59 (s, 9H, 4-*Me*), δ 4.45 (q, 6H, *CH_2*Me), δ 7.10 (d, 3H, *Im*). ^{31}P NMR (CD_2Cl_2): δ −97.89. UV−vis (dichloromethane, nm (M^{-1} cm^{-1})): 330 sh (5100).

[Cu^I(T1Et4MeIP)]Cl (1-Cl). Equimolar amounts of solid CuCl (0.06 g) and T1Et4MeIP (0.20 g, 0.56 mmol) were placed in a 100 mL Schlenk flask, which was subsequently evacuated for 10 min. The flask was then flushed with Ar and charged with 20 mL of dry, degassed acetone via cannula and the resulting mixture stirred at room temperature. A brilliant yellow precipitate formed almost immediately. The reaction mixture was stirred for 1 h, and the precipitate was then collected by filtration under an Ar atmosphere. The yellow powder was dried under a flow of Ar. Yield: 0.21 g. Anal. Calcd for $CuC_{18}H_{27}N_6PCl$: C, 47.25; H, 5.96; N, 18.37. Found: C, 46.82; H, 5.94; N, 17.79. ^1H NMR (CD_2Cl_2): δ 1.27 (t, 9H, CH_2*Me*), δ 1.34 (s, 9H, 4-*Me*), δ 4.21 (q, 6H, *CH_2*Me), δ 6.77 (d, 3H, *Im*). ^{31}P NMR (CD_2Cl_2): δ −106.44. UV−vis (methanol, nm (M^{-1} cm^{-1})): 310 sh (4300).

{[Cu(T1Et4MeIP)]$_2$(O_2)}X_2 (X = PF_6, ClO_4, CF_3SO_3) (2-X). Method A. In a 100 mL Schlenk flask were placed 0.56 mmol (0.20 g) of T1Et4MeIP and an equimolar amount of [(Cu^I(CH_3CN)$_4$]X. The flask was subsequently evacuated for 10 min under a full vacuum, after which an Ar blanket was introduced. O_2-free dichloromethane (10 mL) was added via cannula, and the resulting solution was immediately cooled to −78 °C with stirring. Dry dioxygen was then bubbled vigorously through the colorless solution, and a rapid color change (less than 10 min) to a deep purple was observed. After 30 min of O_2-bubbling, approximately 20 mL of diethyl ether, previously cooled to −78 °C, was added to the solution via cannula, which induced precipitation of a pale purple product. Once a small amount of solid was observed, the solution was allowed to stand for 15 min at −78 °C. The solid was then filtered through a Schlenk frit under a dry Ar atmosphere by gravity and allowed to dry on the frit for 12 h in a −80 °C freezer. The solid PF_6^- and $CF_3SO_3^-$ complexes were found to be stable for several days at room temperature, under argon atmosphere, whereas the solid ClO_4^- complex decomposed within 1 h at room temperature to a green solid.

Method B. A 0.08 mmol sample of [Cu^I(T1Et4MeIP)]X (X = PF_6 (0.045 g), ClO_4 (0.040 g), CF_3SO_3 (0.045 g)) was placed in a 100 mL Schlenk flask and evacuated for 10 min. Dichloromethane (10 mL) was then added via cannula under an Ar atmosphere, and the flask was immediately cooled to −78 °C. A steady stream of dry O_2 was bubbled through the colorless solution, which was kept at −78 °C. Over a period of 5 h, the solution gradually turned to a pale purple suspension. Dry, degassed diethyl ether (50 mL), precooled to −78 °C, was then added to the mixture, which caused precipitation of an additional amount of purple solid. The reaction mixture was then filtered under gravity at −78 °C. Elemental analyses for the PF_6^- and $CF_3SO_3^-$ salts were performed on products obtained via method A. No analysis was obtained on the perchlorate salt, due to its thermal instability over extended periods at room temperature. In acetone-d_6, we generally observed a CH_2Cl_2 ^1H NMR resonance at 5.35 ppm for complexes **2**. (**2**-PF_6)·CH_2Cl_2. Yield: 0.15 g. Anal. Calcd for $Cu_2C_{37}H_{56}N_{12}O_2P_4F_{12}Cl_2$: C, 35.52; H, 4.52; N, 13.44. Found: C, 35.54; H, 4.61; N, 13.54. ^1H NMR (CD_2Cl_2, 213 K): δ 1.32 (s, 9H, CH_2*Me*), δ 2.40 (s, 9H, 4-*Me*), δ 4.37 (s, 6H, *CH_2*Me), δ 7.00 (s, 3H, *Im*). ^{31}P NMR (CD_2Cl_2, 213K): δ −116.37. Resonance raman (514.5 nm laser excitation, KBr, cm^{-1}): 739 ν(O−O). UV−vis (dichloromethane, −78 °C, nm (M^{-1} cm^{-1})): 338 (14 000), 521 (1000). **2**-ClO_4. Yield: 0.09 g. ^1H NMR (CD_2Cl_2, 213 K): δ 1.44 (s, 9H, CH_2*Me*), δ 2.41 (s, 9H, 4-*Me*), δ 4.26 (s, 6H, *CH_2*Me), δ 6.95 (s, 3H, *Im*). ^{31}P NMR (CD_2Cl_2, 213 K): δ −112.05. Resonance raman (514.5 nm laser excitation, KBr, cm^{-1}): 738 ν($^{16}O-^{16}O$), 700 ν($^{18}O-^{18}O$). UV−vis (dichloromethane, −78 °C, nm (M^{-1} cm^{-1})): 338 (20 000), 519 (810). (**2**-CF_3SO_3)·CH_2Cl_2·H_2O. Yield: 0.08 g. Anal. Calcd for $Cu_2C_{38}H_{58}N_{12}O_9P_2F_6S_2Cl_2$: C, 36.67; H, 4.59; N, 13.16. Found: C, 36.67; H, 4.59; N, 13.27. ^1H NMR (CD_2Cl_2, 213 K): δ 1.44 (s, 9H, CH_2*Me*), δ 2.51 (s, 9H, 4-*Me*), δ 4.43 (s, 6H, *CH_2*Me), δ 7.41 (s, 3H, *Im*). ^{31}P NMR (CD_2Cl_2, 213 K): δ −111.99. Resonance raman (514.5 nm laser excitation (KBr, cm^{-1})): 739 ν(O−O). UV−vis (dichloromethane, −78 °C, nm (M^{-1} cm^{-1})): 339 (21 000), 518 (800).

{[Cu(T1Et4MeIP)]$_2$($^{18}O_2$)}(ClO_4)$_2$. This complex was prepared via method A with the following modification. T1Et4MeIP (0.02 g) and an equimolar amount of [(Cu^I(CH_3CN)$_4$]ClO_4 (0.02 g) were reacted as described above; however, the isotopically labeled $^{18}O_2$ was added via syringe (2 mL) and the reaction was stirred at −78 °C for another 1 h and subsequently allowed to sit overnight at that temperature. The product was isolated as outlined in method A.

Dioxygen Complex of [Cu^I(T1Et4MeIP)]Cl (2-Cl). [Cu^I(T1Et-4MeIP)]Cl (0.10 g, 0.22 mmol) was placed in a 100 mL Schlenk flask, and the flask was evacuated under reduced pressure for 15 min. After purging with argon, 20 mL of dry, O_2-free methanol was added to the flask, and the system was immediately cooled with stirring to −78 °C. After 10 min, dry O_2 was bubbled vigorously through the solution, which changed to a purple color within 5 min. The reaction was continued in this manner for 1 h, at which time 30 mL of dry, O_2-free diethyl ether was added to the solution to induce precipitation of the purple complex. The solid was then isolated by gravity filtration at −78 °C. This complex was found to be stable for only minutes as a solid when warmed to approximately −20 °C under an Ar atmosphere. ^1H NMR (CD_3OD, 213 K): δ 1.40 (s, 9H, CH_2*Me*), δ 2.34 (s, 9H, 4-*Me*), δ 4.20 (s, 6H, *CH_2*Me), δ 7.10 (s, 3H, *Im*). ^{31}P NMR (CD_3OD, 213 K): δ −113.89. UV−vis (methanol, −78 °C, nm (M^{-1} cm^{-1})): 322 (9300), 517 (590).

[Cu^I(T1Et4iPrIP)(CH_3CN)]X (X = PF_6, ClO_4, CF_3SO_3) (3-X). T1Et4iPrIP (0.44 mmol, 0.19 g) and equimolar [Cu^I(CH_3CN)$_4$]X were placed in a 100 mL Schlenk flask under argon. O_2-free acetonitrile (20 mL) was added to the flask via cannula with rapid stirring, and the resulting solution was immediately cooled to 0 °C. After 1 h, the stirring was stopped, and the colorless solution was layered with dry O_2-free diethyl ether until a small amount of cloudy white precipitate was observed. The system was then stored at −20 °C overnight, producing a colorless crystalline product. The solvent was decanted, and the colorless product was dried in air. **3**-PF_6. Yield: 0.10 g. Anal. Calcd for $CuC_{26}H_{42}N_7P_2F_6$: C, 45.11; H, 6.13; N, 14.16. Found: C, 45.52; H, 6.29; N, 13.88. ^1H NMR (CD_3OD): δ 1.29 (d, 18H, CH*Me_2*), δ 1.42 (t, 9H, CH_2*Me*), δ 2.24 (s, br, 3H, *CH_3*CN), δ 3.01 (m, 3H, *CH*Me_2), δ 4.21 (m, 6H, *CH_2*Me), δ 7.02 (d, 3H, *Im*). ^{31}P NMR (CD_3OD): δ −112.15, δ −138.65 (sept). UV−vis (methanol, nm (M^{-1} cm^{-1})): 316 sh (3600). (**3**−ClO_4)·2.5 H_2O. Yield: 0.08 g. Anal. Calcd for $CuC_{26}H_{47}N_7PClO_{6.5}$: C, 45.13; H, 6.86; N, 14.17. Found: C, 45.13; H, 6.46; N, 13.88. ^1H NMR (CD_3OD): δ 1.29 (d, 18H, CH*Me_2*), δ 1.41 (t, 9H, CH_2*Me*), δ 2.16 (s, br, 3H, *CH_3*CN), δ 3.03 (m, 3H, *CH*Me_2), δ 4.33 (m, 6H, *CH_2*Me), δ 7.07 (d, 3H, *Im*). ^{31}P NMR (CD_3OD): δ −111.89. UV−vis (methanol, nm (M^{-1} cm^{-1})) 318 (3900). **3**-CF_3SO_3. Yield: 0.07 g. Anal. Calcd for $CuC_{27}H_{42}N_7PSF_3O_3$: C, 46.57; H, 6.09; N, 14.08. Found: C, 46.52; H, 6.12; N, 14.10. ^1H NMR (CD_3OD): δ 1.29 (d, 18H, CH*Me_2*), δ 1.42 (t, 9H, CH_2*Me*), δ 2.34 (s, br, 3H, *CH_3*CN), δ 3.01 (m, 3H, *CH*Me_2), δ 4.34 (m, 6H, *CH_2*Me), δ 7.02 (d, 3H, *Im*). ^{31}P NMR (CD_3OD): δ −112.26. UV−vis (methanol, nm (M^{-1} cm^{-1})): 321 sh (3000).

[Cu^I(T1Et4IPrIP)]Cl (3-Cl). Equimolar amounts of CuCl (0.06 g) and T1Et4iPrIP (0.24 g, 0.56 mmol) were reacted in acetone as described above for the preparation of [Cu(T1Et4MeIP)]Cl. A yellow solution formed immediately, and the stirring was continued for 0.5 h with no discernible precipitation. Diethyl ether was then introduced into the flask (approximately 30 mL) until a yellow powder was observed. This mixture was allowed to stand for 1 h, and the yellow solid was subsequently collected by gravity filtration. ^1H NMR spectra showed a resonance at 2.06 ppm, which we assign to residual acetone in the product. (**3**-Cl)·C_3H_6O. Yield: 0.22 g. Anal. Calcd for $CuC_{27}H_{45}N_6OPCl$: C, 54.06; H, 7.58; N, 14.01. Found: C, 53.58; H, 7.75; N, 13.39. ^1H NMR (CD_3OD): δ 1.24 (d, 18H, CH*Me_2*), δ 1.32 (t, 9H, CH_2*Me*), δ 2.13 (s, br, 3H, *Me_2*CO), δ 3.12 (m, 3H, *CH*Me_2), δ 4.48 (m, 6H, *CH_2*Me), δ 7.00 (d, 3H, *Im*). ^{31}P NMR (CD_3OD): δ −106.58. UV−vis (methanol, nm (M^{-1} cm^{-1})): 318 (sh 3000).

{[Cu(T1Et4iPrIP)]$_2$(O_2)}X_2 (X = PF_6, ClO_4, CF_3SO_3, Cl) (4-X). [Cu^I(T1Et4iPrIP)(CH_3CN)]X or [Cu^I(T1Et4iPrIP)]Cl, (0.07 mmol) was placed in a 100 mL Schlenk flask, and the flask was placed under vacuum for 10 min. O_2-free methanol (10 mL) was added under argon, and this mixture was immediately cooled to −78 °C with stirring. Dry dioxygen was then bubbled through the colorless solution, and rapid transformation to a pale purple color was observed within 5 min. The oxygenation was continued for a total of 30 min at −78 °C, at which time 20 mL of dry, diethyl ether, precooled to −78 °C, was introduced via cannula. The resulting purple powder was collected by gravity filtration overnight in a −80 °C freezer. This solid could be stored for several days at −80 °C without noticeable decomposition. Rapid decomposition (within 5 min) of the solid occurred above −20 °C, which prevented elemental analysis and preparation of reliable samples for resonance Raman spectra. For NMR samples, deuterated methanol was used as the solvent and the corresponding preparation was carried out in situ in a standard NMR tube under Ar. **4**-PF_6. ^{1}H NMR (CD_3-OD, 208 K): δ 1.29 (s, 18H, CH*Me*$_2$), δ 1.41 (s, 9H, CH_2*Me*), δ 2.07 (s, br, 3H, *CH_3*CN), δ 3.49 (s, 3H, *CH*Me$_2$), δ 4.36 (s, 6H, *CH_2*Me), δ 7.42 (s, 3H, *Im*). ^{31}P NMR (CD_3OD, 208 K): δ −114.07, δ −139.04 (sept). UV−vis (methanol, −78 °C, nm (M^{-1} cm^{-1})) 338 (7800), 546 (680). **4**-ClO_4. ^{1}H NMR (CD_3OD, 208 K): δ 1.29 (s, 18H, CH*Me*$_2$), δ 1.39 (s, 9H, CH_2*Me*), δ 2.06 (s, br, 3H, *CH_3*CN), δ 3.47 (s, 3H, *CH*Me$_2$), δ 4.36 (s, 6H, *CH_2*Me), δ 7.38 (s, 3H, *Im*). ^{31}P NMR (CD_3-OD, 208 K): δ −114.02. UV−vis (methanol, −78 °C ,nm ($M^{-1}cm^{-1}$)) 338 (16 000), 546 (940). **4**-CF_3SO_3. ^{1}H NMR (CD_3OD, 208 K): δ 1.29 (s, 18H, CH*Me*$_2$), δ 1.41 (s, 9H, CH_2*Me*), δ 2.04 (s, br, 3H, *CH_3*-CN), δ 3.49 (s, 3H, *CH*Me$_2$), δ 4.36 (s, 6H, *CH_2*Me), δ 7.42 (s, 3H, *Im*). ^{31}P NMR (CD_3OD, 208 K): δ −114.15. UV−vis (methanol, −78 °C, nm (M^{-1} cm^{-1})) 341 (10 000), 541 (800). **4**-Cl. ^{1}H NMR (CD_3OD, 208 K): δ 1.19 (s, 18H, CH*Me*$_2$), δ 1.44 (s, 9H, CH_2*Me*), δ 3.49 (s, 3H, *CH*Me$_2$), δ 4.39 (s, 6H, *CH_2*Me), δ 7.42 (s, 3H, *Im*). ^{31}P NMR (CD_3OD, 208 K): δ −113.90. UV−vis (methanol, −78 °C, nm (M^{-1} cm^{-1})) 340 (12 000), 542 (650).

UV−Vis Absorption/Thermal Cycling. An ≈1.2 mM solution of [Cu^I(L)]X (L = T1Et4MeIP or T1Et4iPrIP) was prepared in a Schlenk flask according to the procedures described above. The solution was then transferred via cannula to a quartz optical dewar (model SK-8506111, with a 1 cm path length, manufactured by William A. Sales, Ltd., Wheeling, II) whose sample chamber had previously been dried under vacuum and purged with argon. After obtaining a UV−vis absorption spectrum, the temperature of the solution in the sample chamber was lowered to −78 °C via a dry ice/acetone bath and dry O_2 was bubbled through the solution in the sample chamber via cannula. A UV−vis absorption spectrum of the resulting purple solution was obtained at −78 °C. The temperature of the solution was then raised rapidly by replacing the dry ice/acetone bath with room temperature acetone. A UV−vis spectrum was obtained at the higher temperature (≈−20 °C), during which an argon stream was passed over the solution via cannula. The solution was then immediately cooled back to −78 °C with a dry ice/acetone bath and O_2 reintroduced as described above. This thermal cycling was repeated as necessary with UV−vis absorption spectra being obtained at the lower and higher temperatures of each cycle.

Physical Measurements. ^{1}H and ^{31}P NMR spectra were measured on a Bruker AM250 or AM300 MHz spectrometer and referenced to the solvent for ^{1}H NMR (chloroform, 7.26 ppm; acetone, 2.04 ppm; methanol, 3.30 ppm) or triphenylphosphine for ^{31}P NMR (0 ppm). Downfield and upfield shifts are reported in ppm as positive and negative, respectively. UV−vis absorption spectra were obtained on a Perkin-Elmer Model 3840 λ-array spectrophotometer or a Shimadzu UV-2101PC spectrophotometer. Resonance raman spectra were obtained on an Instruments SA Ramanor U1000 spectrometer. The instrument design and experimental technique were described previously.[21] The spectra were obtained at 18 K using a 0.5 nm slit width and an excitation wavelength of 514.9 nm from a Coherent Innova 100 10W Argon ion laser at 400 mW. For resonance Raman spectra, samples of **2**-PF_6 or **2**-ClO_4 were mixed with KBr under an argon stream to produce an approximately 50% pellet by weight. The KBr pellets were prepared and loaded in the Raman spectrometer within 2−3 min. This short time frame was found to be essential due to the hygroscopic nature and thermal instability of the sample pellets, particularly that of the perchlorate salt.

Table 1. Crystallographic Data for [Cu(TlEt4iPrIP)(CH_3CN)](PF_6) (**3**-PF_6)

formula	$CuC_{26}H_{42}N_7P_2F_6$	Z	8
fw	692.25	ϱ_{calcd}, g cm^{-3}	1.359
space group	$I2_13$	λ(Cu Kα), Å	1.54184
a, Å	18.912(2)	T, °C	23
b, Å	18.912(1)	μ, cm^{-1}	23.0
c, Å	18.912(2)	transm coeff	0.929−0.995
β, deg	90	$R(F_o)$	7.5
V, Å^3	6765.1(9)	$R_w(F_o)$	9.8

Table 2. Atomic Positional Parameters for [Cu(TlEt4iPrIP)(CH_3CN)](PF_6) (**3**-PF_6)[a]

atom	x	y	z	B (Å^2)
Cu	0.237	0.237	0.237	3.539(9)
P1	0.485	0.485	0.485	6.62(3)
P2	0.339	0.339	0.339	3.10(1)
F1	0.495	0.566	0.485	18.1(5)
F2	0.399	0.468	0.493	24.5(8)
N1	0.2001(3)	0.3282(4)	0.2855(3)	3.5(1)
N2	0.2157(3)	0.4218(3)	0.3538(3)	3.3(1)
N3	0.179	0.179	0.179	3.87(6)
C1	0.145	0.145	0.145	3.86(8)
C2	0.102	0.102	0.102	4.93(9)
C11	0.2467(4)	0.3645(4)	0.3244(4)	3.1(1)
C12	0.1484(4)	0.4213(4)	0.3323(5)	4.1(2)
C13	0.1383(5)	0.3643(5)	0.2923(5)	3.7(2)
C14	0.2495(6)	0.4767(5)	0.3980(5)	5.0(2)
C15	0.4590(6)	0.1478(8)	0.268(1)	9.8(4)
C16	0.0711(5)	0.3368(6)	0.2560(6)	5.1(2)
C17	0.0042(7)	0.376(1)	0.2815(8)	9.4(4)
C18	0.0788(7)	0.3450(8)	0.1754(6)	6.7(3)

[a] Anisotropically refined atoms are given in the form of the isotropic equivalent displacement parameter defined as ($^4/_3$)[$a_2B(1,1) + b_2B(2,2) + c_2B(3,3) + ab(\cos\gamma)B(1,2) + ac(\cos\beta)B(1,3) + bc(\cos\alpha)B(2,3)$].

X-ray Structure Determination of [Cu^I(T1Et4iPrIP)(CH_3CN)]-PF_6 (3-PF_6). Crystals were grown by layering an acetonitrile solution of the compound with diethyl ether and allowing for slow diffusion at −20 °C. A suitable colorless crystal of dimensions 0.2 × 0.2 × 0.2 mm was mounted on the end of a glass fiber and sealed in epoxy resin. Data collection was carried out on an Enraf-Nonius CAD4 diffractometer equipped with a graphite crystal monochromator using Cu Kα radiation (λ = 1.541 84 Å) at 23 °C. The orientation matrix and least squares analysis were calculated over 25 machine-centered reflections (15° < 2θ < 25°). Pertinent crystallographic details are listed in Table 1. Three intensity control reflections were measured every 156 reflections with no appreciable decay. The crystal was initially observed to be *I* centered cubic, and reflections were omitted according to *hkl* ($h + k + l = 2n$). The solution was then placed in the space group $I2_13$ by the systematic absence $h00$ ($h = 2n$). The initial atom solution was solved by direct methods using SIR88.[22] All other atoms except C1 were located by successive difference Fourier maps and refined isotropically by successive least squares refinement. Cu, N1, P1, P2, F1, and F2 were all located by difference map and refined with fixed positional parameters. C1 was not observed in the difference map and was placed by calculation and refined isotropically. All atoms were eventually anisotropically refined in the final least squares matrix to produce the final result. Non-Poisson weights modified by the Dunitz−Seiler technique were used in the final cycle of least squares.[23] Tables 1−3 contain the crystallographic data. Table S1 contains values of $10|F_o|$ and $10|F_c|$ and Table S2 contains thermal parameters.

X-ray Absorption Data Collection and Analysis. Two samples,

(21) Drozdzewski, P. M.; Johnson, M. K. *Appl. Spectrosc.* **1988**, *42*, 1575.

(22) Burla, M. C.; Camalli, M.; Cascarano, G.; Giacovazzo, G.; Polidori, G.; Spagna, R.; Viterbo, D. *J. Appl. Crystallogr.* **1989**, *22*, 389.

(23) Dunitz, J. D.; Seiler *Acta. Crystallogr.* **1973**, *B29*, 589.

Table 3. Bond Lengths (Å) and Bond Angles (deg) for [Cu(TlEt4iPrIP)(CH_3CN)](PF_6) (**3**-PF_6)

atom 1	atom 2	distance	atom 1	atom 2	distance
Cu	N1	2.075(8)	N2	C12	1.34(1)
Cu	N3	1.901(0)	N2	C14	1.48(1)
P1	F1	1.541(0)	N3	C1	1.101(0)
P1	F2	1.659(0)	C1	C2	1.416(0)
P2	C11	1.828(8)	C12	C13	1.33(1)
N1	C11	1.34(1)	C13	C16	1.53(1)
N1	C13	1.36(1)	C16	C17	1.54(2)
N2	C11	1.35(1)	C16	C18	1.54(2)

atom 1	atom 2	atom 3	angle	atom 1	atom 2	atom 3	angle
N1	Cu	N3	122.7(2)	P2	C11	N1	124.9(6)
F1	P1	F2	108.0(0)	P2	C11	N2	124.5(6)
Cu	N1	C11	116.6(5)	N1	C11	N2	110.6(8)
Cu	N1	C13	138.4(6)	N2	C12	C13	108.4(8)
C11	N1	C13	104.9(8)	N1	C13	C12	109.7(8)
C11	N2	C12	106.4(7)	N1	C13	C16	120.0(8)
C11	N2	C14	127.4(8)	C12	C13	C16	130.3(9)
C12	N2	C14	126.1(8)	C13	C16	C17	112.0(1)
CU	N3	C1	180.0(0)	C13	C16	C18	109.0(1)
N3	C1	C2	180.0(0)	C17	C16	C18	110.0(1)

Table 4. X-ray Absorption Spectroscopic Data Collection and Reduction Information

monochromator crystal	Si[220]
energy resolution, eV	≈1
detection method	transmission
detector type	ionization chamber (N_2)
scan length, min	21
no. of scans in average	8
temperature, K	10
energy standard	Cu foil (first inflection)
energy calibration, eV	8980.3
E_0, eV	9000
pre-edge background energy range, eV (polynomial order)	9050−9689(2)[a]
spline background energy range, eV (polynomial order)	9029−9200(2) 9200−9400(3) 9400−9689(3)

[a] Background was calculated from fitting this (EXAFS) region, then a constant was substracted so that the background matched the data just before the edge.

one containing the bis(ligand) complex, [Cu^{II}(T1Et4MeIP)$_2$](PF_6)$_2$,[24] and the other, the dioxygen adduct, {[Cu(T1Et4MeIP)]$_2$(O_2)}(CF_3SO_3)$_2$ (**2**-CF_3SO_3), were each mixed with approximately 50% KBr, then pressed into a homogeneous pellet. Data were collected at the Stanford Synchrotron Radiation Laboratory, beamline VII-3, and were reduced using the XFPAK software package.[25] Other relevant data collection and reduction information is listed in Table 4. Curve-fitting analyses of the EXAFS data required consideration of multiple scattering by the imidazole groups and used EXCURVE.[26] Positioning of the T1Et4MeIP ligand in the simulation of the **2**-CF_3SO_3 EXAFS was modeled on the basis of the EXAFS of [Cu^{II}(T1Et4MeIP)$_2$](PF_6)$_2$.[24] Only the distances and Debye-Waller factors for the Cu−O and Cu- - -Cu interactions were optimized in the final curve fitting for **2**-CF_3SO_3.

Results and Discussion

Synthesis and Structures of [Cu^I(T1Et4RIP)(CH_3CN)](X) (R = Me, iPr; X = PF_6, ClO_4, CF_3SO_3) (3-X). The Cu^I complexes were synthesized via stoichiometric Lewis acid−base reactions between T1Et4RIP and [Cu^I(CH_3CN)$_4$]X. Due to solubility constraints, the complexes with T1Et4MeIP were synthesized in methanol, and upon complexation, essentially

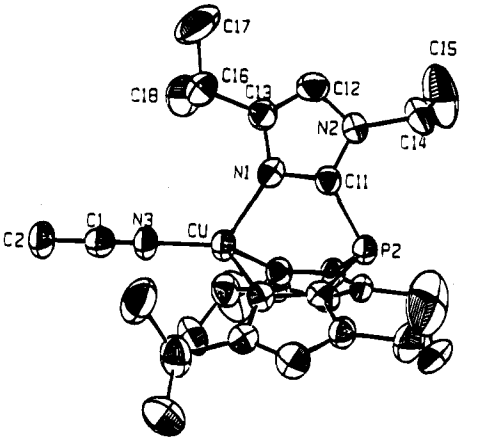

Figure 1. ORTEP diagram of the copper complex in [Cu^I(T1Et-4iPrIP)(CH_3CN)]PF_6 (**3**-PF_6) showing the atom labeling scheme.

Scheme 2

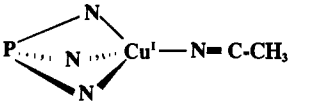

pure [Cu^I(T1Et4MeIP)]X (**1**-X) instantly precipitated from solution. The stoichiometry and spectroscopy for **1**-X indicated no solvent coordination to the copper. ^{31}P NMR proved especially convenient for determination of the T1Et4RIP:PF_6 stoichiometry in both **1**-PF_6 and **3**-PF_6. Integrated areas of the T1Et4RIP singlet vs the PF_6^- septet were found to be approximately 1:1 in these complexes. Although **1**-X could be a bridged dimeric species analogous to those observed for hydrotris(pyrazolyl)boratocopper(I) complexes,[27,28] X-ray crystallography of **1**-PF_6 recrystallized from acetonitrile (**1**-PF_6·CH_3CN) revealed a mononuclear complex with one tridentate T1Et4MeIP and a coordinated acetonitrile.[24] This donor ability of acetonitrile apparently suppresses any tendency toward dimer formation by [Cu^I(T1Et4MeIP)]$^+$ and stabilizes a mononuclear trigonally distorted tetrahedral coordination geometry around Cu^I, as illustrated schematically in Scheme 2. The preceding statements also apply to the more sterically encumbered [Cu^I(T1Et4iPrIP)(CH_3CN)]X (**3**-X) complexes, which were found to be readily prepared in acetonitrile and precipitated by addition of ether. Subsequent recrystallization gave X-ray quality crystals. The crystal structure of **3**-PF_6 is presented in Figure 1, and selected bond lengths and angles are summarized in Table 3. A crystallographically imposed 3-fold rotation axis passes through the copper atom, the apical ligand phosphorus, and the acetonitrile ligand. The structure was solved by placement of the copper atom by Patterson interpretation and subsequent refinement on a least-squares difference map. All non-hydrogen atoms of the ligated solvent molecule were placed by intensity difference maps except for C1 and N3, which were ghost atoms. From spectral and analytical data, the presence of an acetonitrile molecule was indicated and the intermolecular distances were calculated according to the structural data from **1**-PF_6·CH_3CN.[24] These acetonitrile atoms were then placed in calculated positions and held fixed at 0.333 occupancy while allowing their thermal parameters to vary. The structures of **1**-PF_6·CH_3CN and **3**-PF_6 are nearly identical in the significant

(24) Lynch, W. E.; Kurtz, Newton, M. G.; Scott, R. A.; Wang, S. To be submitted for publication.
(25) Scott, R. A. *Methods Enzymol.* **1985**, *117*, 414.
(26) Strange, R. W.; Blackburn, N. J.; Knowles, P. F.; Harris, S. S. *J. Am. Chem. Soc.* **1987**, *109*, 7157.
(27) (a) Carrier, S. M.; Ruggiero, C. E.; Tolman, W. B. *J. Am. Chem. Soc.* **1992**, *114*, 4407. (b) Carrier, S. M.; Ruggiero, C. E.; Houser, R. P,; Tolman, W. B. *Inorg. Chem.* **1993**, *32*, 4889.
(28) Mealli, C.; Arcus, C. S.; Wilkinson, J. L.; Marks, T. J.; Ibers, J. A. *J. Am. Chem. Soc.* **1976**, *98*, 711.

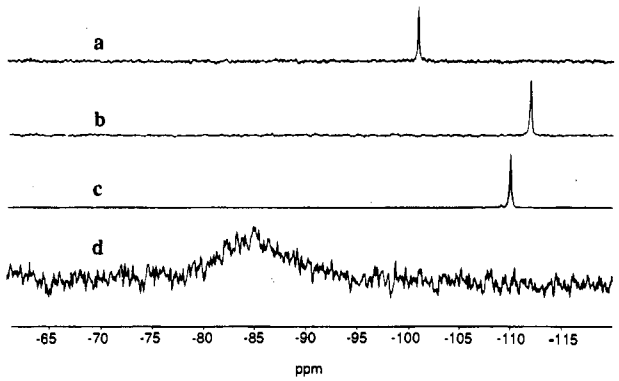

Figure 2. ^{31}P NMR data in CD_2Cl_2 for (a) $[Cu^{I}(T1Et4MeIP)](ClO_4)$ (**1**-ClO_4) at 20 °C ($\delta = -99$ ppm), (b) $\{[Cu(T1Et4MeIP)]_2(O_2)\}(ClO_4)_2$ (**2**-ClO_4) at −65 °C (δ = -112 ppm), (c) the thermal decomposition product from (b) after 1 h at 20 °C (δ = -109 ppm), and (d) the thermal decomposition product, $[Cu^{II}(T1Et4MeIP)_2](ClO_4)_2$, from (b) after 7 d at 20 °C ($\delta = -56$ ppm).

distances and angles. Cu−N(Im) and Cu−$NCCH_3$ bond distances in **3**-PF_6 are 2.08 and 1.901 Å, respectively, compared to 2.07 and 1.90 Å in **1**-PF_6·CH_3CN.[24] The (Im)N−Cu−$NCCH_3$ angles are 122.7° for **3**-PF_6 and 123.2° for **1**-PF_6·CH_3CN.[24] These distances and angles are similar to those observed for $[Cu^{I}(PPh_3)(HB(3,5\text{-}Me_2pz)_3)]$, which contains the tridentate HB-(3,5-$Me_2pz)_3$(1−) ligand with PPh_3 occupying the fourth coordination site.[9]

Reactions of the Cu^{I} Complexes with Dioxygen. Low-temperature exposure of the Cu^{I} complexes to an atmosphere of excess dry O_2, as described in the Experimental Section, produced complexes formulated as $[(LCu)_2(O_2)]X_2$ (L = T1Et4MeIP (**2**-X) or T1Et4iPrIP (**4**-X)). Two methods were used to produce **2**-X. In situ assembly of Cu^{I} complexes **1**-X from equimolar T1Et4MeIP and $[Cu^{I}(CH_3CN)_4]X$ in dichloromethane followed by exposure of the resulting solution to dry dioxygen at −78 °C resulted in nearly instantaneous formation of the purple O_2 adduct, **2**-X. Exposure of the preisolated Cu^{I} complexes, **1**-X, to dry dioxygen at −78 °C in methanol also resulted in **2**-X, but in lower yield and purity than for the in situ method. Both methods of oxygenation gave the purple product at temperatures as high as −30 °C, but for convenience and greater stability, −78 °C was generally used. Isolation of the solid O_2 adducts, **2**-X, was achieved by addition of degassed diethyl ether at −78 °C to initiate precipitation of the purple solid. The solid was then collected by gravity filtration in a fritted Schlenk-type filter under an argon atmosphere placed in a −80 °C freezer. The solid product could be manipulated under an argon atmosphere at room temperature for short periods and stored at −20 °C indefinitely. Addition of dry dioxygen to solutions of **1**-X at temperatures greater than −30 °C resulted in irreversible oxidation of the Cu^{I} species to an unidentified green complex. The preformed complexes **1**-X could be dimeric, as discussed above, or alternatively may have the counterion, X, weakly coordinated. Either of these alternatives would explain the longer reaction times and lower yields of **2**-X starting from preformed **1**-X relative to the in situ method. The NMR resonances of **2**-X were not noticeably broader than those of **1**-X (cf. Figure 2), which, together with the small (<0.5 ppm) differences in ^1H NMR chemical shifts (cf. the Experimental Section) indicate that the O_2 adducts **2**-X are approximately diamagnetic.

Oxygenation of the Cu^{I} complexes **3**-X containing the more sterically demanding T1Et4iPrIP ligand to produce $\{[Cu(T1Et4iPrIP)]_2(O_2)\}X_2$ (**4**-X), proceeded in a manner similar to that for complexes **1**-X/**2**-X. Due to solubility constraints, methanol rather than dichloromethane was used as the solvent for **3**-X, and oxygenations of this complex were generally carried out at −78 °C. Under these conditions, oxygenation of **3**-X required approximately three times longer to reach completion than did oxygenation of **1**-X prepared in situ in dichloromethane. At concentrations necessary to perform ^1H and ^{31}P NMR experiments, solutions of the purple O_2 adduct **4**-X in CD_3OD at 208 K invariably showed NMR resonances assigned to both **4**-X and the starting Cu^{I} complex **3**-X, indicating incomplete oxygenation of **3**-X. The NMR resonances of **4**-X were not noticeably broader than those of **3**-X, which together with the small (<0.5 ppm) differences in ^1H NMR chemical shifts between **3**-X and **4**-X (cf. the Experimental Section) indicate that the O_2 adducts **4**-X are approximately diamagnetic. The longer oxygenation times of **3**-X vs **1**-X and the apparently incomplete oxygenation of **3**-X but not **1**-X (except for X = Cl, discussed below) could be due to greater steric restrictions of the iPr vs Me group in the T1Et4iPrIP vs T1Et4MeIP ligand or to competition of O_2 with the more readily coordinating methanol solvent used for oxygenation of **3**-X. Isolation of solid O_2 adducts, **4**-X, was achieved as described above for **2**-X, but unlike **2**-X, the solid **4**-X could not be manipulated above −20 °C without rapid decomposition even under a dry argon atmosphere.

When solutions of O_2 adducts **2**-X were allowed to warm rapidly to room temperature under an O_2 atmosphere, irreversible decomposition through an intermediate green species (within 5 min) to a paramagnetic aqua-blue complex occurred over the course of days. This process was readily monitored by ^{31}P NMR, which gave characteristic resonances corresponding to four distinct, consecutive species (cf. Figure 2): (a) the starting Cu^{I} complex, (b) the purple, oxygenated complex, (c) an (apparently) diamagnetic, kelly-green complex, and (d) the final paramagnetic, aqua-blue complex. This last complex was determined by X-ray crystallography to be the bis(ligand)copper-(II) complex, $[Cu(T1Et4MeIP)_2]^{2+}$.[24,29] The high-temperature limit for formation of a stable (i.e., long-lived) dioxygen adduct, **4**-X, which contains the T1Et4iPrIP ligand, was found to be −60 °C. As described below, this temperature limit did not prevent *rapid* temperature cycling between **4**-X at −78 °C and **3**-X at ≈−20 °C. As with **2**-X, dioxygen adducts **4**-X, when *rapidly* warmed to room temperature, also showed irreversible formation of a kelly-green complex within minutes. However, in this case, the green species was the terminus of the thermal decomposition path. The green species resulting from decomposition of **4**-X appeared to be quite similar to the green intermediate obtained during thermal decomposition of **2**-X. Both green species gave sharp ^1H and ^{31}P NMR signals, indicative of diamagnetism. In $[Cu^{II}(T1Et4MeIP)_2]^{2+}$, the 4-methyl substituents on the imidazolyl rings of the two ligands are essentially in van der Waals contact. The larger 4-iPr substituents apparently prevent formation of the analogous bis-(ligand)copper(II) complex with T1Et4iPrIP. The kelly-green, apparently diamagnetic, species have properties closely resembling those described by Kitajima et al.,[30] for carbonato-bridged hydrotris(3,5-di-R-pyrazolyl)boratodicopper(II) complexes (R = Me, iPr), the source of carbonate being atmospheric CO_2. Such complexes are described as "forest-green" with a much smaller residual paramagnetism at room temperature than other possible candidates, such as the "blue-green" μ-oxo- or "blue" bis(μ-

(29) X-ray crystallographic data for $[Cu(T1Et4MeIP)_2](PF_6)_2$: *P*1 (no. 2); $Z = 2$; Cu−N1(Im), 2.04 Å; Cu−N2(Im), 2.04 Å; Cu−N3(Im), 2.35Å , $R = 0.070$, $R_w = 0.105$. The EXAFS data on this complex, when fit to the scattering contributions of the imidazolyl ligands calculated from the X-ray crystallographic data, yielded a goodness-of-fit value of 0.038.

(30) Kitajima, N.; Hikichi, S.; Tanaka, M.; Moro-oka, Y. *J. Am. Chem. Soc.* **1993**, *115*, 5496.

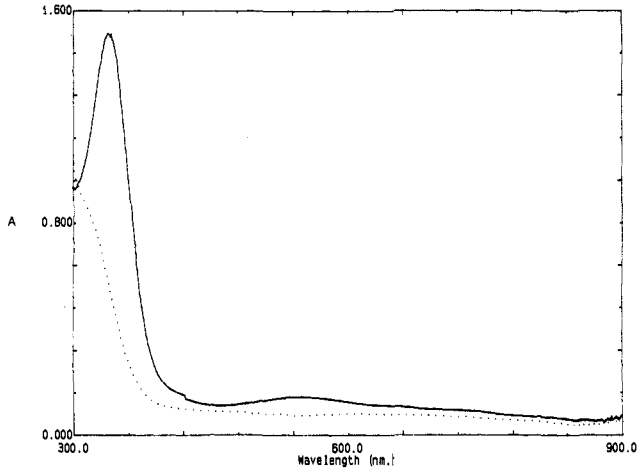

Figure 3. UV−vis absorption spectra of a 0.40 mM methanol solution of the $[Cu^{I}(T1Et4iPrIP)(CH_3CN)]PF_6$ (**3**-PF_6) (dotted line) and the dioxygen adduct $\{[Cu(T1Et4iPrIP)]_2(O_2)\}(PF_6)_2$ (**4**-PF_6) (solid line) obtained at −78 °C.

hydroxo)dicopper(II) complexes.[6,9,30] As described below, the most significant difference found between complexes **1**-X and **3**-X was reversible O_2 binding by the latter.

Visible Absorption Spectra of the Dioxygen Adducts 2-X and 4-X. The colorless solutions of Cu^{I} complexes, **1**-X or **3**-X, turned dark purple upon exposure to dry dioxygen at low temperature. The absorption spectra of the purple, oxygenated solutions are attributed to the O_2 adducts **2**-X and **4**-X. Figure 3 presents the absorption spectrum of $[Cu^{I}(T1Et4iPrIP)(CH_3CN)](PF_6)$ (**3**-PF_6) and the resultant spectrum upon oxygenation with dry dioxygen in dry methanol giving **4**-PF_6. These spectra are quite similar to those of **1**-X and **2**-X, respectively. The absorption spectra for **2**-X contain peaks at 519 nm (ϵ = 800−1000 M^{-1} cm^{-1}) and 339 nm (ϵ = 20000 M^{-1} cm^{-1}). These absorptions closely resemble those of $[Cu(HB(3,5\text{-}R_2pz)_3)]_2(O_2)$ at 530−551 nm ($\epsilon \approx$ 900 M^{-1} cm^{-1}) and 338−350 nm ($\epsilon \approx$ 20 000 M^{-1} cm^{-1}),[7] where they have been assigned as $O_2^{2-} \rightarrow Cu^{II}$ charge transfer transitions.[1,4,11] As mentioned in the Introduction, the same assignments have been given to similar absorptions for oxyhemocyanin. Spectra of complexes **2**-X and **4**-X also exhibit a shoulder at ≈680 nm (better seen in Figure 6, discussed below). Similar features have been assigned to d−d transitions in spectra of $[Cu(HB(3,5\text{-}R_2pz)_3)]_2(O_2)$ and oxyhemocyanin.[1,4,11] The somewhat lower molar absorptivities obtained for O_2 adducts **4**-X vs **2**-X (cf. the Experimental Section) could be due to incomplete oxygenation of **3**-X, as mentioned above for the NMR solutions.

Resonance Raman Spectra of $\{[Cu(T1Et4MeIP)]_2(O_2)\}$-$X_2$ (2-X). Approximately 50% KBr pellets of **2**-X were excited using the 514.5 nm Ar laser line, which falls underneath the ≈520 nm absorption band of these complexes. Using natural isotopic abundance O_2 ($^{16}O_2$), all complexes **2**-X exhibited a resonance Raman band at ≈740 cm^{-1}. Figure 4 shows the resonance raman spectra of **2**-ClO_4 using $^{16}O_2$ and $^{18}O_2$. The $\Delta\nu(^{16}O_2-^{18}O_2)$ = 38 cm^{-1} is close to the value of 42 cm^{-1} calculated for an O−O harmonic oscillator. Detailed analyses of Raman and IR spectra of $[Cu(HB(3,5\text{-}R_2pz)_3)]_2(O_2)$ (R = iPr, Ph) have resulted in assignment of similar frequencies (741 cm^{-1} (R = iPr), 763 cm^{-1} (R = Ph)) and $\Delta\nu(^{16}O_2-^{18}O_2)$ (40−43 cm^{-1}) to ν(O−O) of peroxo in the planar $\mu-\eta^2:\eta^2$-bridging geometry, and furthermore, these frequencies and isotope shifts appear to be diagnostic of such a geometry.[1c,4b,11] This essentially pure O−O stretching frequency is also close to that observed for oxyhemocyanin (750 cm^{-1}).[4] Due to the relatively rapid

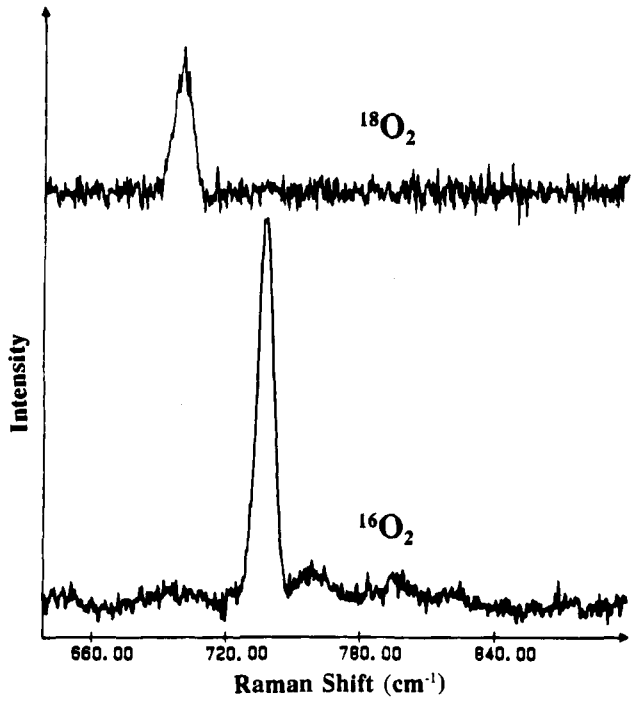

Figure 4. Resonance Raman spectra of $\{[Cu(T1Et4MeIP)]_2(O_2)\}(ClO_4)_2$ (**2**-ClO4) prepared at −78 °C in CH_2Cl_2 with $^{16}O_2$ or $^{18}O_2$ and pressed into 50% KBr pellets. Spectra were obtained at 18 K using 514.5 nm laser excitation.

decomposition of solid complexes **4**-X, we have so far been unable to obtain their Raman spectra.

EXAFS Analysis of $\{[Cu(T1Et4MeIP)]_2(O_2)\}(CF_3SO_3)_2$ (2-CF_3SO_3). X-ray absorption spectroscopic analyses of the bis(ligand) complex $[Cu^{II}(T1Et4MeIP)_2](PF_6)_2$ and the dioxygen adduct $\{[Cu(T1Et4MeIP)]_2(O_2)\}(CF_3SO_3)_2$ (**2**-CF_3SO_3) were performed on 50% KBr samples. Approximate values for the scattering contribution of three imidazolyl ligands per Cu^{II} in **2**-CF_3SO_3 were calculated from correlations of the X-ray crystallographic and EXAFS data on the bis(ligand)Cu^{II} complex.[24,29] Analysis of the EXAFS data on **2**-CF_3SO_3 was then carried out using these calculated scattering contributions with the Cu−N(Im) distances held fixed at 2.05 and 2.30 Å. The resulting distances for all ligand atoms in **2**-CF_3SO_3 are tabulated in Table 5. Figure 5 shows the raw EXAFS data and Fourier transforms for **2**-CF_3SO_3 (solid lines) and the best simulations (dashed lines). Chemically reasonable Cu−O (1.94 Å) and Cu−Cu′ (3.48 Å) distances result from the analysis. The goodness-of-fit value for this fit (0.045) becomes significantly worse (0.050) if the Cu′ scatterer is omitted. The interatomic distances listed in Table 5 agree well with those reported for the X-ray crystal structure of $[Cu(HB(3,5\text{-}i\text{-}Pr_2pz)_3)]_2(O_2)$, including the Cu-O (1.90 Å) and Cu−Cu′ (3.56 Å) distances and two sets of Cu-N distances (2.00 and 2.26 Å).[7] This latter complex contains a planar Cu_2O_2 core with a symmetric $\mu-\eta^2:\eta^2$-bound O_2. An alternative O_2-binding mode in **2**-CF_3SO_3 could be *trans*-(μ-1,2), as observed in the X-ray crystal structure of $[(LCu)_2(O_2)]^{2+}$, where L = tris[(2-pyridyl)methyl]amine.[31] However, both the Cu−Cu′ distance (4.34 Å) and ν(O−O) (840 cm^{-1}) for this latter complex are significantly different from those determined in this study for **2**-CF_3SO_3. Therefore, the EXAFS structural results on **2**-CF_3SO_3 are represented in Scheme 3 in terms of a planar $\mu-\eta^2:\eta^2$ O_2-bridging geometry, although our present data do not rule out small deviations from a planar Cu_2O_2 structure. It is noteworthy that all of the structural features in Scheme 3,

(31) Tyeklár, Z.; Jacobson, R. R.; Wei, N.; Murthy, N. N.; Zubieta, J.; Karlin, K. D. *J. Am. Chem. Soc.* **1993**, *115*, 2677.

Table 5. EXCURVE Curve-Fitting Results for Cu EXAFS of $[Cu(TlEt4MeIP)]_2(O_2)(CF_3SO_3)_2$ (**2**-CF_3SO_3)[a]

group	shell[b]	N_s	R_{as} (Å)	σ_{as}^2 (Å^2)	f' [c]
Im	Cu–N3	(2)	2.05	0.0055	0.045
Im	Cu–C2		2.95	0.075	
Im	Cu–C4		3.15	0.0075	
Im	Cu–N1		4.16	0.0095	
Im	Cu–C5		4.25	0.0095	
Im	Cu–N3	(1)	2.30	0.0045	
Im	Cu–C2		3.13	0.0070	
Im	Cu–C4		3.46	0.0070	
Im	Cu–N1		4.39	0.0085	
Im	Cu–C5		4.56	0.0090	
	Cu–P	(1)	3.46	0.0035	
	Cu–C	(3)	3.56	0.0090	
	Cu–O	(2)	1.94	0.0040	
	Cu–Cu′	(1)	3.48	0.0140	

[a] Group is the chemical unit defined for the multiple scattering calculation. N_s is the number of scatterers (or groups) per copper; R_{as} is the copper-scatterer distance; σ_{as}^2 is a mean square deviation in R_{as}. [b] Atom numbering for carbons and nitrogens of TlEt4MeIP is shown in Scheme 1. [c] f' is a goodness-of-fit statistic normalized to the overall magnitude of the $k^3\chi(k)$ data:

$$f' = \frac{\{\sum[4k^3(\chi_{obsd}(i) - \chi_{calcd}(i))]^2/N\}^{1/2}}{(k^3\chi)_{max} - (k^3\chi)_{min}}$$

where N is the number of data points.

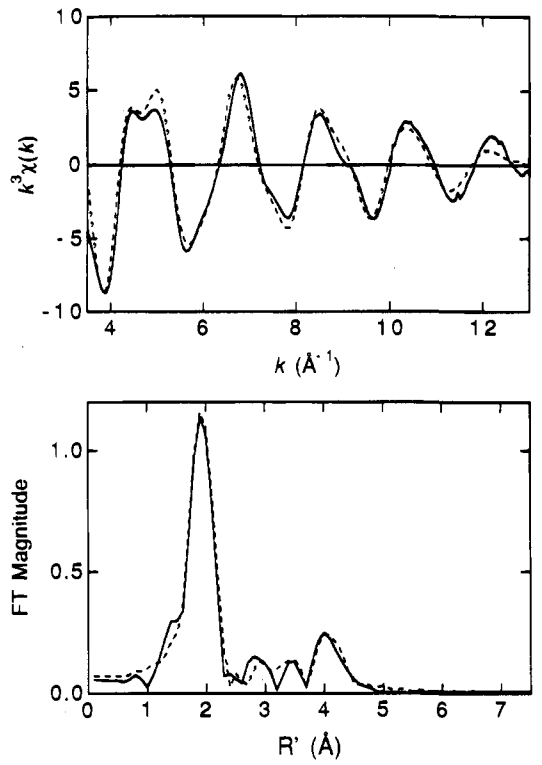

Figure 5. Cu EXAFS data (top) and Fourier transform (bottom) for $\{[Cu(TlEt4MeIP)]_2(O_2)\}(CF_3SO_3)_2$ (**2**-CF_3SO_3). Solid lines represent the experimental data; dashed lines correspond to the simulation described in the text and Table 5.

including the two sets of Cu–N(Im) distances, reflect those observed in the X-ray crystal structure of oxyhemocyanin.[12]

Reversible Dioxygen Binding by Copper(I) Complexes 3-X. Dry dichloromethane solutions of $[Cu^I(TlEt4MeIP)]^+$ (**1**-X) bind O_2 rapidly to give **2**-X at temperatures below −50 °C, as judged by formation of the purple complex. Upon warming above −20 °C, the spectrum of **2**-X apparently reverts to that of the starting Cu^I complex. However, the apparently reformed Cu^I complex could not be taken through additional O_2 binding cycles. Instead, as described above, rapid decomposition

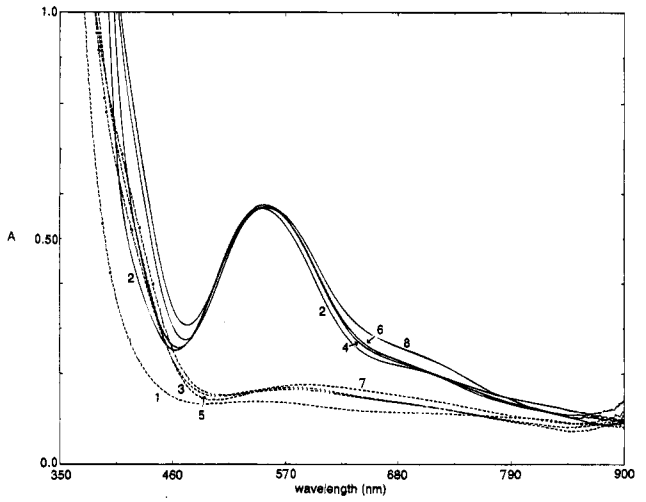

Figure 6. UV–vis absorption spectra of a 1.2 mM methanol solution of $[Cu^I(TlEt4iPrIP)(CH_3CN)]ClO_4$ (**3**-ClO_4) (dashed curves) and the dioxygen adduct $\{[Cu(TlEt4iPrIP)]_2(O_2)\}(ClO_4)_2$ (**4**-ClO_4) $\lambda_{max} = 546$ (solid curves) obtained during temperature cycling between −78 and approximately −20 °C, as described in the text. Numbers indicate chronological order of the spectra.

Scheme 3

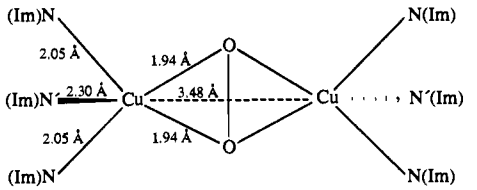

occurred, eventually resulting in the bis(ligand) complex $[Cu^{II}(TlEt4MIP)_2]^{2+}$. Evacuation of solutions of **2**-X at −78 °C failed to remove bound O_2, as judged by retention of the purple color. Methanolic solutions of $[Cu^I(TlEt4iPrIP)(CH_3CN)]X$ (**3**-X) oxygenate similarly, although somewhat more slowly, to yield the purple adduct at temperatures of < −65 °C. Thermal cycling between −78 °C and approximately −20 °C results in the set of spectra shown in Figure 6, which indicates interconversion between **3**-ClO_4 and **4**-ClO_4. The starting spectrum of **3**-ClO_4 (spectrum 1) was obtained at room temperature. The sample was then cooled to −78 °C and dioxygen added to produce **4**-X (spectrum 2). Warming the solution rapidly (approximately 2 min) resulted in conversion back to **3**-ClO_4 (spectrum 3). After obtainment of spectrum 3, the solution was immediately recooled to −78 °C. Dry dioxygen was then added to the mixture at −78 °C until oxygenation was complete (15–30 min), resulting in spectrum 4. Spectra for two more of these cycles are shown in Figure 6 (spectra 5–8). For X = PF_6, ClO_4, and CF_3SO_3, this thermal cycling appeared to be reversible for at least 10 cycles, when conducted as described in the Experimental Section. During this cycling, there was no observable shift or decrease in intensity of the characteristic absorption maximum at ≈546 nm for the O_2 adduct, although a gradual increase in absorption below 460 nm was noted, which could be indicative of a minor portion of concomitant irreversible oxidation. Given the structural and spectroscopic data presented above, the reversible **3**-X/**4**-X interconversion can reasonably be formulated as the equilibrium in eq 2 with the

$$2[Cu^I(TlEt4iPrIP)]^+ + O_2 \leftrightarrow \{[Cu(TlEt4iPrIP)]_2(O_2)\}^{2+} \quad (2)$$

product having the μ–η^2:η^2-peroxo-bridging Cu_2O_2 structure

depicted in Scheme 3. In the case of **3**-Cl, the extent of reversibility of O_2 binding under these conditions was found to be much less than 50% upon cycling from the lower to higher temperatures and back. **3**-Cl was found to be much more prone to irreversible oxidation as either a solid or solution at ambient temperatures than were **3**-PF_6, **3**-ClO_4 or **3**-CF_3SO_3. Chloride may compete relatively effectively compared to the other anions with both O_2 for LCu^I and peroxide for LCu^{II}. The terminal oxidation product of **3**-Cl is an unidentified paramagnetic brown complex rather than the diamagnetic green species described above for oxidation of the other **3**-X.

While several other Cu^I complexes have been reported to bind O_2 reversibly,[1,32] the $[Cu(HB(3,5\text{-}R_2pz)_3)]_2(O_2)$ complexes, which appear to most closely resemble those described here, are *not* reported to be reversible. Thus, other than oxyhemocyanin,[12] the complexes **4**-X are apparently the first reported examples of copper-dioxygen complexes with the planar (or nearly so) μ-η^2:η^2-peroxo Cu_2O_2 geometry to exhibit reversible O_2 binding (see Note Added in Proof). Although it is tempting to attribute the reversibility of O_2 binding to the presence of imidazolyl rather than pyrazolyl ligands, the fact that the complexes **1**-X/**2**-X are not found to be interconvertible under our conditions makes a such conclusion tenuous at best. The contrast in reversibility between **1**-X/**2**-X vs **3**-X/**4**-X could be due to any of several factors including steric, electronic, and solvent effects.[33] The steep temperature dependence of the **3**-X/**4**-X interconversion can be attributed to a strongly negative reaction entropy for formation of the 2:1 $[LCu]^+$:O_2 adduct, as depicted in eq 2.[34] This unfavorable entropy is apparently overcome in hemocyanin by fixing the two Cu^I centers in close proximity, thereby promoting O_2 binding at room temperature.

Summary and Conclusions

Solutions of $[Cu^I(T1Et4RIP)]^+$ form diamagnetic O_2 adducts at ≤ -60 °C exhibiting spectroscopic characteristics of planar (μ-η^2:η^2-peroxo)dicopper(II) complexes, particularly an unusually low O−O stretching frequency ($\approx$740 cm^{-1}) and intense absorptions at 520−546 nm and $\approx$340 nm attributable to peroxo-to-copper(II) charge transfer transitions. EXAFS measurements on $\{[Cu(T1Et4MeIP)]_2(O_2)\}(CF_3SO_3)_2$ gave Cu−Cu′ (3.5 Å) and Cu−O (1.94 Å) distances consistent with the μ-η^2:η^2-peroxo-bridging geometry in a planar Cu_2O_2 unit and inconsistent with a *trans*-(μ-1,2)-peroxo-bridging geometry. These distances plus the two sets of Cu−N(Im) distances (2.05 and 2.30 Å) in this complex are quite similar to those in oxyhemocyanin. The complexes with R = iPr exhibited reversible O_2 binding upon thermal cycling between −78 and $\approx$−20 °C. Thus, copper complexes of T1Et4RIP (R = Me, iPr) have been successfully used to model spectroscopic, magnetic, structural, and functional features of the dicopper site in hemocyanin.

Acknowledgment. Dr. M. G. Newton assisted in X-ray crystallographic structure determination, Dr. J. S. Harwood in NMR data collection and interpretation, and Professor M. K. Johnson and Mr. Brian Crouse in Raman data collection. We thank Professor Thomas Sorrell for sharing his results with us throughout the course of this work and Dr. Vivian A. Vankai for initial explorations of the copper−dioxygen chemistry reported herein. This work was supported by funds made available by the University of Georgia as a result of an NIH Research Career Development Award to D.M.K. (HL02207). Some of the equipment was supported by an NSF Research Training Group Award to the Center for Metalloenzyme Studies (DIR 90-14281).

Supplementary Material Available: Table of anisotropic thermal parameters for **3**-PF_6 (1 page); table of observed and calculated structure factors for **3**-PF_6 (12 pages). This material is contained in many libraries on microfiche, immediately follows this article in the microfilm version of this journal, and can be ordered from the ACS; see any current masthead page for ordering information.

Note Added in Proof. A second example of an apparently planar (μ-η^2:η^2-peroxo)dicopper(II) complex which reversibly binds O_2 was recently reported.[35]

(32) (a) Karlin, K. D.; Nasir, M. S.; Cohen, B. I.; Cruse, R. W.; Kaderli, S.; Zuberbühler, A. D. *J. Am. Chem. Soc.* **1994**, *116*, 1324. (b) Wei, N. W.; Murthy, N.; Tyeklár, Z.; Karlin, K. *Inorg. Chem.* **1994**, *33*, 1177.

(33) We have found that Cu^I complexes of both the less sterically encumbered TMeIP and the more sterically encumbered T1Et4tBuIP do not appear to form O_2 adducts under our conditions.

(34) Karlin, K. D.; Wei, N.; Jung, B.; Kaderlin, S.; Niklaus, P.; Zuberbühler, A. D. *J. Am. Chem. Soc.* **1993**, *115*, 9506.

(35) Mahapatra, S.; Halfen, J. A.; Wilkinson, E. C.; Que, L., Jr.; Tolman, W. B. *J. Am. Chem. Soc.* **1994**, *116*, 9785.